

Simulation of adsorbate-induced faceting on curved surfaces.

Daniel Niewieczerzał and Czesław Oleksy*

Institute of Theoretical Physics, University of Wrocław, Plac Maksa Borna 9, 50-204 Wrocław, Poland

A simple solid-on-solid model, proposed earlier to describe overlayer-induced faceting of bcc(111) surface, is applied to faceting of curved surfaces covered by an adsorbate monolayer. Surfaces studied in this paper are formed by a part of sphere around the [111] pole. Results of Monte Carlo simulations show that the morphology of a faceted surface depends on the annealing temperature. At an initial stage the surface around the [111] pole consists of 3-sided pyramids and step-like facets, then step-like facets dominate and their number decreases with temperature, finally a single big pyramid is formed. It is shown that there is a reversible phase transition at which a faceted surface transforms to an almost spherical one. It is found that the temperature of this phase transition is an increasing function of the surface curvature. Simulation results show that measurements of high temperature properties performed directly and after fast cooling down to a low temperature lead to different results.

PACS numbers: 68.35.Rh, 68.43.De, 64.60.Cn, 68.35.Bs, 68.60.Dv

I. INTRODUCTION

It has been recently demonstrated that ultrathin metal films induce faceting of bcc(111) surfaces. Atomically rough W(111) and Mo(111) surfaces, when covered by a single physical monolayer of certain metals (Pd, Rh, Ir, Pt, Au) and annealed to $T > 700\text{K}$, undergo massive reconstruction from a planar morphology to a microscopically faceted surface^{1,2,3,4,5,6,7}. In most of investigated bcc(111) surfaces, the faceted morphology comprises 3-sided pyramids with {211} facets and facet sizes ranging from ~ 3 to 100 nm. It has been shown that the metal that induces the faceting acts like a surfactant and remains on the surface during the faceting transformation⁷.

Suggestions that faceting in these systems is thermodynamically favorable have been confirmed by first-principles calculations^{7,8,9} performed for (111), (211), and (110) surfaces of Mo and W. Results show lowering of the surface energy as surfaces are being covered by metal overlayer (e.g. Pd, Pt, Au). Moreover, at coverage of one physical monolayer, the bcc(111) surface becomes unstable against faceting, i.e. the system gains energy by transition from (111) to {211} orientation.

Interesting results have been obtained for faceting on curved surfaces of W and Mo in FIM (field ion microscopy)^{10,11,12} and FEM (field emission microscopy) experiments^{13,14,15}. Initially a spherical surface comprises macroscopic crystal facets. After depositing a metal film (e.g. Pd, Pt) or oxygen layer and annealing at elevated temperatures, an increase of the macroscopic {110} and {211} crystal facets is observed. An unexpected change in the faceted morphology occurs near the <111> poles, where step-like {211} microfacets are formed^{10,11}. The number of step-like facets decreases with the annealing temperature, and in some cases, a sin-

gle {211} pyramid around the [111] pole is observed¹¹. Moreover, occurrence of new facets {123}, {178} in Pt on W and Pd on Mo has been reported in papers on FEM^{14,15}.

In theoretical studies of complicated surface problems (e.g. roughening transition, surface reconstruction, surface growth, surface phase transitions) simple models like lattice gas models or solid-on-solid (SOS) models are applied^{16,17,18,19,20,21,22,23,24,25,26}. In our earlier paper²⁷ we have proposed a SOS model to study the adsorbate-induced faceting of the bcc(111) crystal surface at constant coverage. Monte Carlo simulation results show formation of pyramidal facets in accordance with experimental observations. Moreover, the model describes a reversible phase transition from a faceted surface to a disordered (111) surface. Such a phase transition has been found in the Pd/Mo(111) system³. In this paper we study faceting of a curved bcc crystal surface by using the SOS model. We focus on changes in surface morphology in the vicinity of the [111] pole, where step-like {211} facets were observed in FIM experiments. The paper is organized as follows. In Sec. II the SOS model for a curved surface of a bcc crystal is described. Results of Monte Carlo simulations, including changes in the surface morphology with the annealing temperature, and a reversible phase transition, are presented in Sec. III.

II. THE SOS MODEL

To study an adsorbate-induced faceting on a spherical surface we use a solid-on-solid model of Ref.²⁷ that describes faceting of bcc(111) surface. Let us recall the main assumptions. Atoms along the closed packed direction [111] form columns which are represented in the SOS model by their positions on the (111) plane, $i = (i_x, i_y)$, and heights, h_i . Column positions form a triangular lattice (see Fig. 1) which is obtained by projection of the bcc crystal lattice on the (111) plane. Each column comprises substrate atoms and one adsorbate atom at

*Corresponding author.

Electronic address: oleksy@ift.uni.wroc.pl

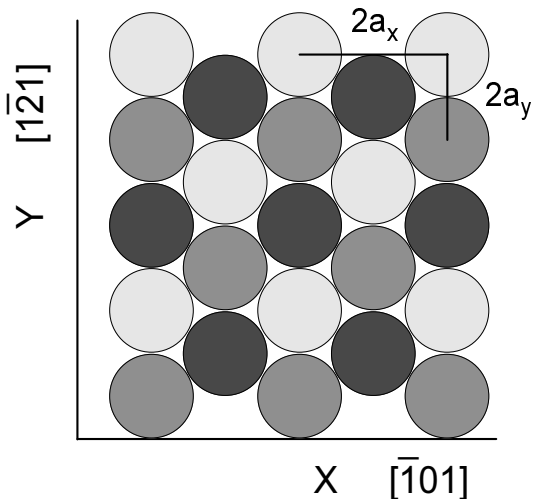


FIG. 1: Schematic top view of the bcc(111) surface. Atoms from three successive geometrical layers represent positions of columns in the SOS model. The Z axis is normal to the (111) plane and $a_x = a\sqrt{2}/2$, $a_y = a\sqrt{6}/6$.

$$\begin{aligned}
 H = \frac{1}{2} \sum_i \left\{ \sum_{j_1} [J_1 \delta(|h_i - h_{j_1}| - 1) + K_1 \delta(|h_i - h_{j_1}| - 2)] + \sum_{j_2} [2J_2 \delta(|h_i - h_{j_2}|) + (2J_2 + K_2) \delta(|h_i - h_{j_2}| - 3)] \right. \\
 \left. + J_2 \sum_{j_3} [\delta(|h_i - h_{j_3}| - 2) + \delta(|h_i - h_{j_3}| - 4)] \right\} + NJ_0, \quad (1)
 \end{aligned}$$

where the sums over j_1 , j_2 , and j_3 represent the sums over first, second, and third neighbours of the column at site i , respectively. Model parameters J_0 , J_1 , J_2 , K_1 , and K_2 can be expressed by interaction energies between substrate and adsorbate atoms (for details see²⁷).

A. Initial conditions for spherical surfaces

We assume that the surface has a initially spherical shape determined by the radius R and the angular radius θ (see Fig. 2). The integer values of column heights, h_i , that minimize a deviation from the perfect spherical shape, are chosen. Positions of columns on the (111) plane form a circle of radius $R_x = R \sin \theta$. We choose fixed boundary conditions, i.e., outside the circle the columns form the (111) face and their heights are frozen. Such boundary conditions make calculations much easier because the number of interaction constants in Hamiltonian (1) can be reduced to one, as will be shown in what follows. It is worth noting that we can also study a flat (111) surface by an appropriate choice of initial col-

umn heights in the circle. This implies a constant coverage of 1 physical monolayer. There is also a restriction imposed on column heights: the nearest neighbour column heights can differ only by $\pm 1, \pm 2$. A surface atom represented in the model by (i_x, i_y, h_i) has a position $(i_x a_x, i_y a_y, h_i a_z)$ in the bcc crystal, where a_z is the distance between neighbouring (111) layers ($a_z = a\sqrt{3}/6$) and a is the lattice constant. The model Hamiltonian represents surface formation energy which depends on column heights h_i in the following form

umn heights in the circle. In this way we can compare adsorbate-induced faceting of flat and curved surfaces³⁰ using the same conditions, i.e. the annealing temperature, annealing Monte Carlo time, the number of surface atoms, and the boundary conditions. The restriction imposed on column heights of the nearest neighbours (see Sec. II) limits the angular radius to $\theta \leq 20^\circ$. An example of a spherical surface with $\theta = 20^\circ$ is shown in Fig. 3, where a (111) facet and {211} facets occur together with terraces. There are also smaller facets with higher Miller indices. It is worth noting that in all surface images shown in this paper, the color of a surface atom represents the number of its nearest neighbours with smaller heights. Such representation allows an easy identification of different facets, e.g. {110} facets are represented by value 3 and row, trough of {211} facets by 5,1, respectively. Investigation of faceting of curved tungsten surface induced by palladium¹⁰ has revealed that step-like microfacets are formed in (111) crystal zones. Hence, the present model will be used to study faceting around the single [111] pole on a spherical surface.

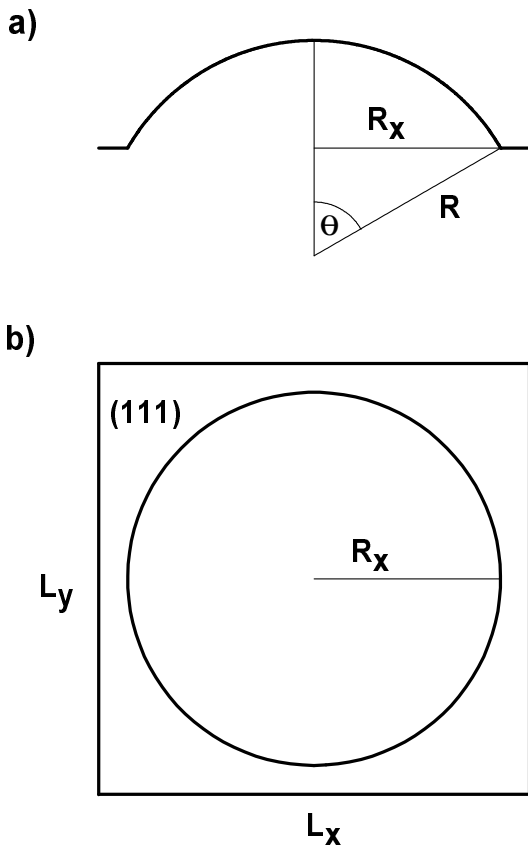


FIG. 2: Schematic (a) side view (b) top view of a spherical surface.

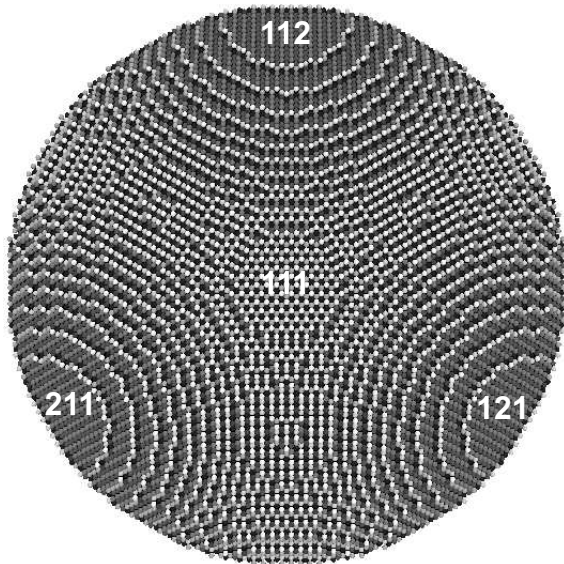


FIG. 3: Top view of a spherical surface. The color of a surface atom represents the number of its nearest neighbours (NN) with smaller heights. The brightest color is for 6 NN and the darkest one for 0 NN.

B. Energy of spherical surface

In Ref.²⁷ it has been shown that energies per column of ideal faces (111), (211), and (110) are the same for the interactions limited to the nearest neighbours. It turns out that the same is true for the energy of a spherical surface. We calculated the number of bonds between nearest neighbours: b_1 with $|\Delta h| = 1$ and b_2 with $|\Delta h| = 2$ for hundreds of angles θ from the interval $[0^\circ, 20^\circ]$ and for constant number of columns N . For most of the angles, b_1 and b_2 are exactly the same as in the case of the ideal (111) surface ($\theta = 0^\circ$). For a few angles the values of b_1 and b_2 are a little changed e.g., $|\Delta b_1|/b_1 = 3.8 \times 10^{-4}$ for $R_x = 93a_x$ ($N = 23497$) and $|\Delta b_1|/b_1 = 5.6 \times 10^{-5}$ for $R_x = 370a_x$ ($N = 327367$), and such angles will be omitted. On the other hand, permitted changes of a configuration conserve b_1 and b_2 . Thus the energy of the nearest neighbours interactions is conserved in this SOS model and it can be neglected (or treated as the reference energy). For this reason we can limit the number of the model parameters to two (J_2, K_2). Similarly as in²⁷, we can eliminate one more parameter by choosing J_2 as the unit of energy. We will work with dimensionless quantities: energy $\tilde{H} = H/J_2$, temperature $\tilde{T} = k_B T/J_2$, and interaction constant $K = K_2/J_2$ (in what follows, the tilde will be omitted). It has been shown that the energy of the (211) face is minimal when $-2 < K < 0$, whereas the (111) surface is stable for $K > 0$. Therefore simulations of a flat SOS model²⁷ with negative K (e.g. $K = -1.25$) show faceting of a bcc(111) surface. In the present model, energy of a spherical surface E_{sp} decreases with θ for negative K but is still greater than the energy of a (211) face, e.g. the energy per column for $K = -1.25$ are: $E_{111} = 7$, $E_{sp}(\theta = 20^\circ) = 6.26$ and $E_{211} = 5.75$. Thus we expect that a spherical surface may undergo faceting after annealing at an elevated temperature. In this paper we performed all calculations for $K = -1.25$ for two reasons. First, the same value was already used in faceting of a bcc(111) surface²⁷, so one can compare results for two different models. Second, we estimated the value of K for the Pd on W(111) system using surface formation energies from Fig. 3 in Ref.⁷ and the relations between E_{hkl} and the model parameters²⁷. As the first-principle calculations⁷ were performed both with the local-density approximation (LDA) and with the generalized gradient approximation (GGA), we obtained two different values of K : -1.06 with LDA and -1.25 with GGA. We finally chose the latter because the GGA is considered as more reliable than LDA⁷.

III. MONTE CARLO SIMULATIONS

Properties of the spherical SOS model with constant coverage are investigated by Monte Carlo (MC) simulation in canonical ensemble using standard Metropolis algorithm^{28,29}. A new configuration is generated by choosing two lattice sites i and j and changing heights of

columns at these sites: $(h_i, h_j) \rightarrow (h_i - 3, h_j + 3)$. This is equivalent to moving a substrate atom from a site i to a site j . The new configuration is accepted with probability $p = \min(1, \exp(-\delta E/kT))$, where δE is the energy change of the system generated by transition to a new configuration. In the simulations we measure the mean energy $\langle H \rangle$, the heat capacity

$$C_V = (\langle H^2 \rangle - \langle H \rangle^2) / k_B T^2, \quad (2)$$

and the mean-square width of the surface,

$$\delta h^2 = \left\langle \frac{1}{Na^2} \sum_j (h_j - \langle h \rangle)^2 \right\rangle. \quad (3)$$

The latter quantity depends also on the curvature radius, therefore we introduce the mean-square radial deviation

$$\delta r^2 = \left\langle \frac{1}{Na^2} \sum_j (r_j - R)^2 \right\rangle \quad (4)$$

where r_j is distance of a surface atom j from the center of the sphere.

A. Faceting of curved surfaces

In this section we investigate changes of a surface covered by a physical monolayer of adsorbate during the warming up and cooling down processes. Simulations start at a temperature T_0 , with the spherical surface determined by the radius R and the angle θ (see section II A). The warming up process is characterized by gradual elevation of temperature, $T_i = T_{i-1} + \Delta T$. At each temperature the system is annealed for time τ , measured in Monte Carlo steps per site (MCS). After reaching the maximal temperature, the system starts to cool down by changing $\Delta T \rightarrow -\Delta T$. In order to measure the temperature dependence of interesting quantities we choose 1000 configurations in the final stage at each temperature and we repeat the warming up – cooling down cycle for 20 samples. In what follows we will explain why averaging over samples is important in this problem.

Results of simulations carried out for $K = -1.25$, $R_x = 93a_x$, $\theta = 20^\circ$, $\Delta T = 0.03$ and $\tau = 2 \times 10^5$ are presented in Figs. 4 – 9. The temperature dependence of δr^2 in the warming up – cooling down cycle clearly shows (see Fig. 4) that this process is irreversible. For $T > 0.3$ the mean-square radial deviation increases as the temperature is elevated, which indicates that $\{211\}$ facets are formed on initially spherical surface. First we observe two types of facets on the surfaces (see Fig. 5(a) and Fig. 6): 3-sided pyramids and pits located near the pole, and elongated facets forming steps between the $\{211\}$ faces. The steps are built of two alternating facets, e.g. (211) and (121). They have characteristic parallel long edges, oriented along $\langle 311 \rangle$ directions, that can be seen in FIM experiments^{10,11} as bright lines. Note that

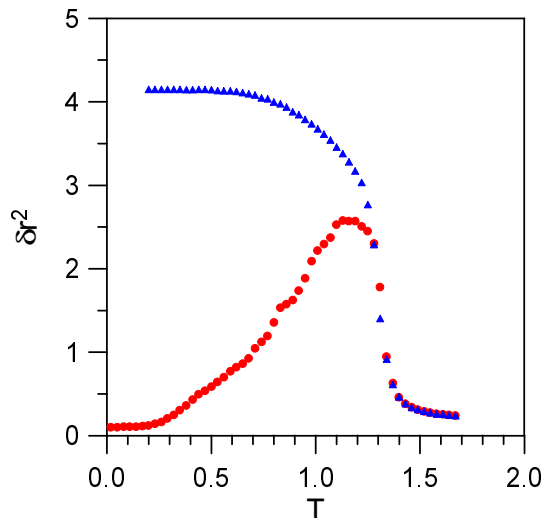


FIG. 4: Temperature dependence of δr^2 during the warming up (red circles) and the cooling down (blue triangles) of the system.

there are also concave edges (dark lines on Fig. 6) which are not present in FIM images. Further increase of the temperature makes the pyramids to disappear and reduces the number of steps (see for example Fig. 5(b)). In other words, a single pyramid with multiple edges is observed. As temperature is increased, even more, the number of these edges is reduced (see Fig. 5(c)). At high enough temperature, it is possible to observe a single 3-sided pyramid on the surface (see Fig. 5(d)); sometimes this pyramid has a double edge. Above $T_d \approx 1.31$, a rapid decline of δr^2 is observed. This indicates a defaceting transition at which the pyramid disappears (see e.g. Fig. 8(a)). Although δr^2 is very small above T_d , the surface is not spherical. We observe also that the surface energy rapidly increases at T_d and the heat capacity attains its maximum. A similar defaceting transition was obtained in simulations of faceting of a bcc(111) surface²⁷ and observed in LEED experiments³ for Pd on Mo(111). The reverse process of slow cooling down the system from the highest temperature, leads again to faceting at the temperature T_d . Hence this is a reversible phase transition.

B. Measurements after fast cooling

In FIM experiment¹¹ the number of parallel edges on a faceted curved surface was measured as a function of the annealed temperature. Because FIM images are taken after a rapid cooling to a low temperature, we adopted a similar procedure to measure the average number of parallel edges, n_e . Configurations chosen at a temperature T were quickly cooled down (the system was held for 20 MCS at each T_i) to the temperature $T_m = 0.2$ at which calculations were performed. This procedure re-

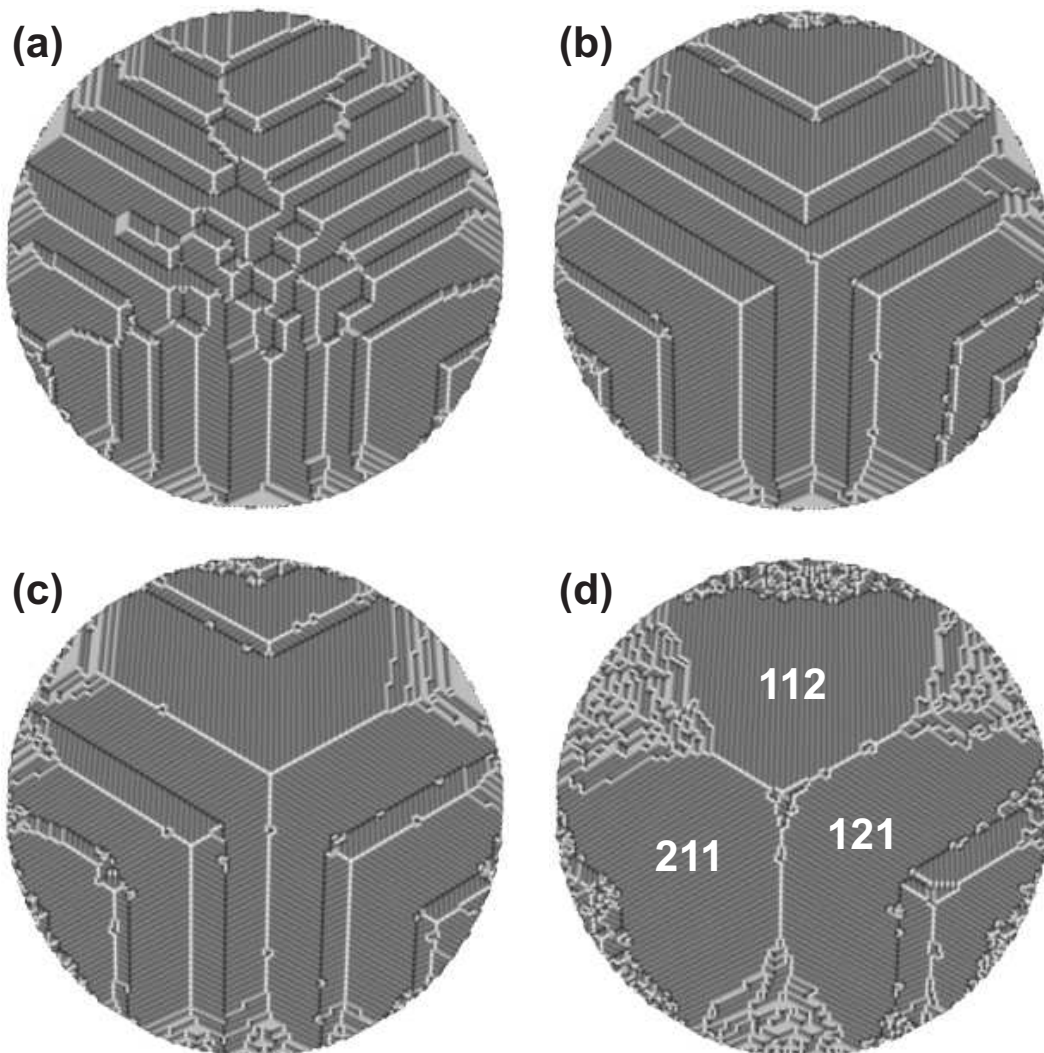


FIG. 5: Top view of the surface after annealing to: (a) $T = 0.41$, (b) $T = 0.68$, (c) $T = 0.86$ and (d) $T = 1.10$.

duces the thermal disorder and makes it possible to use a simple algorithm for edges searching. It is interesting to note that the number of parallel edges decreases with the temperature down to the defaceting temperature and then suddenly increases (see Fig. 7). Similar behavior was observed in the FIM experiment¹¹. The reason why fast cooling can reproduce a pyramid with multiple edges lays in morphology of disordered surface. When the temperature is elevated over T_d , the pyramid is initially damaged near the apex and along the edges. In these regions the surface is not spherical but has a disordered hill-and-valley structure, i.e. there are many small $\{211\}$ facets which form irregular, short $\{211\}$ steps. As the temperature is elevated, the disordered regions broaden (see Fig. 8(a)). On the other hand, fast cooling causes the system to return to a pyramid with multiple edges (see Fig. 8(b)) and multiplicity depends on the width of the disordered region and the cooling rate. This fact can be used to estimate T_d from experimental results, provided that the temperature obtained is below the desorption

temperature. We have also checked how this effect depends on the cooling rate. If the cooling is 10 times faster, then this effect does not occur, i.e. the disordered surfaces remains frozen. In contrast to this, cooling of the disordered phase will result in a big 3-sided pyramid on the surface for cooling rates over hundred times slower.

The quantities like n_e , δr^2 , δh^2 have different temperature behavior for a single sample and when they are averaged over many samples. The single sample temperature dependence of these quantities have step-like character (e.g. see Fig. 9). We think that this effect is connected with large sizes of step-like $\{211\}$ facets on a curved surface. A massive transport of atoms is needed to reduce one convex edge by merging two neighbouring $\{211\}$ steps. Of course, there should be an energy barrier for such process and its height must depend on the size of $\{211\}$ facets. Therefore the width of the plateau occurring in $n_e(T)$ in Fig. 9 increases with the annealing temperature. On the other hand, $n_e(T)$ averaged over many sample becomes a smooth function of temperature

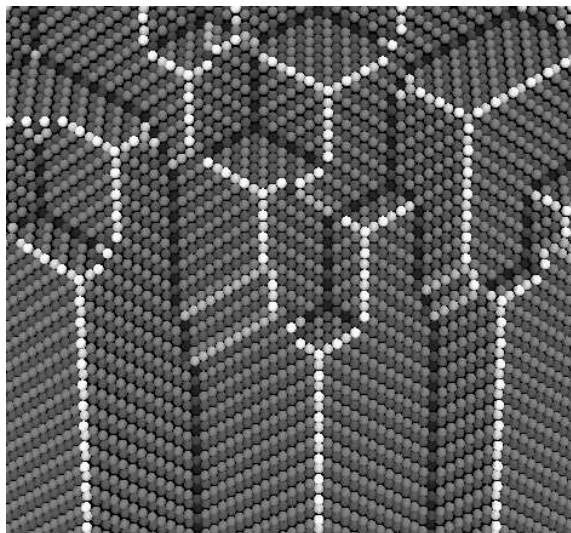


FIG. 6: Enlargement of the central region from Fig. 5(a) where step-like facets and pyramids (pits) coexist.

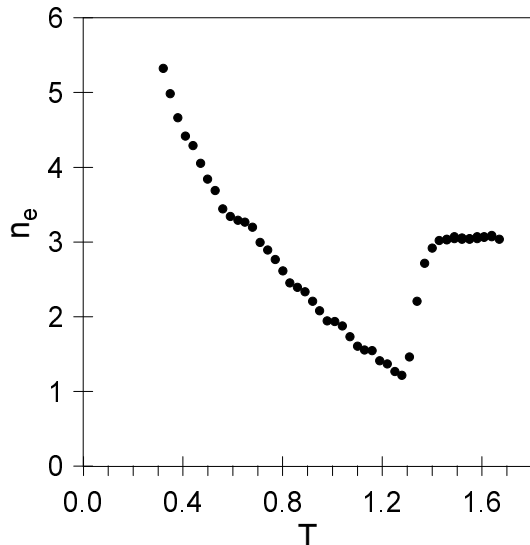


FIG. 7: The average number of parallel edges versus temperature calculated after fast cooling to $T = 0.2$.

because the growth of facets proceeds in individual way for each sample due to the fact that the distances between edges are not constant at a given T (see Fig. 5), but they have visible dispersion.

C. Defaceting of curved surfaces

It has been mentioned in Sec III A that defaceting temperature, T_d , of spherical surface with ($\theta = 20^\circ$) is greater than in the case of a flat surface. To investigate the dependence of T_d on the surface curvature we

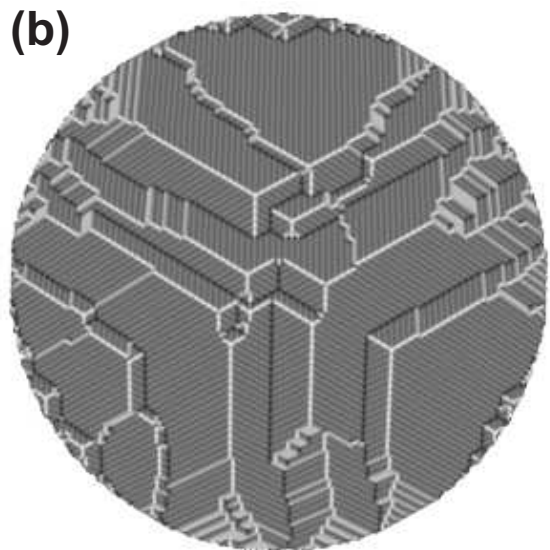
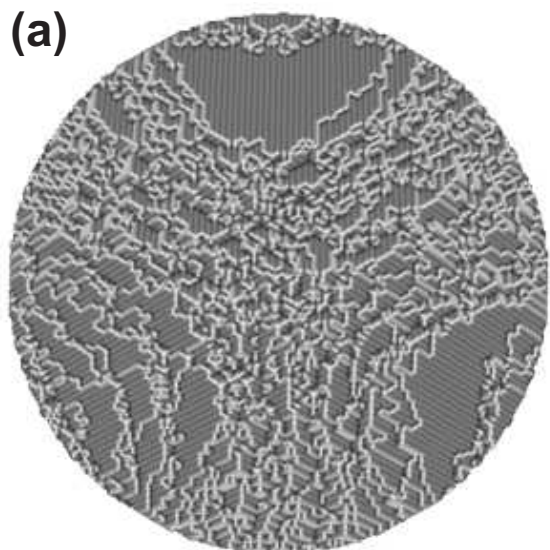


FIG. 8: Snapshot of the surface (a) at $T = 1.4$, (b) after fast cooling from $T = 1.4$ to $T = 0.2$.

performed a series of simulations for several angles θ , keeping the number of columns N (or R_x) fixed. This means that the radius $R = R_x / \sin \theta$ of a spherical surface was varied. Simulation started from a high temperature and as the system was cooled down with $\Delta T = 0.01$, we measured the surface energy, the heat capacity, the mean-square width and the mean-square radial deviation near the reversible phase transition. The system was held at each temperature for 10^6 MCS. We see in Fig.10(a) that the surface energy of a flat surface rapidly decreases at the defaceting temperature T_d . This is the first-order phase transition and the energy difference is equal to the latent heat. Behaviors of E and δh^2 indicate that this phase transition differs from the roughening phase transition^{21,24,25,26} which belongs to the universality class of Kosterlitz-Thouless transition.

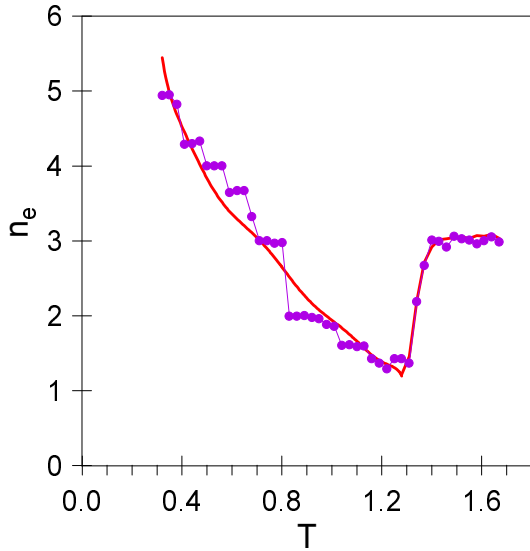


FIG. 9: The number of parallel edges for a single sample (circles) and averaged over 20 samples (the thick line represents data depicted in Fig.7).

It is clearly shown in Fig.10 that the temperature of defaceting transition increases as the curvature of the surface increases. For a surface with $\theta = 20^\circ$ the change of T_d is about 10% with respect to the flat case. We also see that the change of the surface energy at the phase transition decreases with θ . The same behavior is observed in the dependence of δh^2 on T and θ (see Fig.10(b)).

We think that the increase of T_d with θ is related to the entropy reduction in the disordered phase. The surface free energy (SFE), $F = E - TS$, of the faceted phase F_f at the transition temperature T_d is equal to SFE of the disordered phase F_d . Therefore, the temperature of phase transition can be obtained from $T_d(\theta) = \Delta E(\theta, T_d) / \Delta S(\theta, T_d)$, where $\Delta X = X_d - X_f$ for $X = E, S$. As is seen in Fig. 10(a) the change of internal energy ΔE decreases with θ at T_d . Thus the change of entropy ΔS should also be a decreasing function of θ . The decrease of entropy in disordered phase with θ can be justified by the fact that one can observe an increase of $\{211\}$ areas and a contraction of disordered regions on the surface at T_d as curvature (or θ) increases.

IV. DISCUSSION

It is shown that a simple solid-on-solid model can be applied to study adsorbate-induced faceting of the $[111]$ pole region of a spherical surface. Just as in the case of faceting of a bcc(111) surface, it is possible to specify interaction constants that describes a situation when an initially prepared spherical surface covered by a physical monolayer of adsorbate has a surface formation energy greater than $\{211\}$ surfaces. Thus, the faceting of a

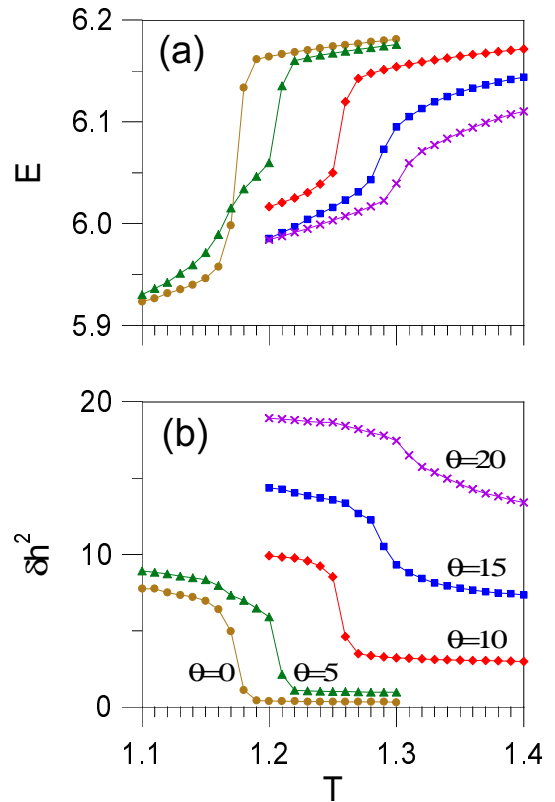


FIG. 10: Dependence of (a) surface energy, (b) square mean width on temperature near faceting - defaceting transition for several angles θ .

curved surface is thermodynamically favorable. Results of Monte Carlo simulations show that the morphology of a faceted surface depends on the annealing temperature. One can distinguish three stages: (1) Formation of 3-sided pyramids around the $[111]$ pole and step-like $\{211\}$ facets between the faces of $\{211\}$ orientations. The latter form long edges observed in FIM experiments^{10,11}. (2) Disappearing of pyramids around the $[111]$ pole and domination of step-like facets whose number decreases with the temperature. (3) Formation of a single large pyramid on the surface. Note that the last two cases were observed in FIM experiments. The first case, a mixture of two kinds of facets, has not been experimentally detected yet. Using our model, we can investigate in detail the structure of a faceted spherical surface. In particular, it is possible to examine properties difficult for experimental studies: concave edges between elongated facets, transition from step-like facets to pyramids and pits, defects, etc.

It is shown that there exists a temperature of faceting - defaceting transition T_d above which disordered regions appear along pyramid edges. Although mean-square radial deviation δr^2 rapidly decreases above T_d , the surface is not spherical. Antczak et al¹⁴ observed in a FEM experiment of Pt on W tip emitter that faceting diminishes

at $T > 1600\text{K}$ and the hemispherical form of the emitter is recovered. As platinum is desorbed from tungsten emitter at temperatures above 1900K ¹⁴, this observation can indicate that defaceting occurs in Pt on W system. It would be interesting to verify experimentally this suggestion. We found that at temperatures just above T_d , disordered regions are not "spherical" but they have disordered hill-and valley structure with many small $\{211\}$ facets which form irregular, short $\{211\}$ steps. This fact seems to be important for measurements of high-temperature properties performed after fast cooling down to a low temperature, a situation typical e.g. in FIM experiments. It is shown that fast cooling may transform the disordered surface into a multi-step surface (see Fig.8(b)). This is manifested in a temperature behavior of the number of parallel edges n_e , which exhibits an unexpected increase above the phase transition temperature T_d (see Fig.7). Similar behavior of n_e has been found for oxygen adsorbed on curved W¹¹. We believe that this fact can be used to determine the temperature of defaceting, provided that T_d is below the desorption temperature (desorption is not included in the model). Formation of facets after a rapid cooling of disordered surface can be explained by a fast massive atomic rearrangement. Such effect has been observed in a Pd/Mo(111) system³

in which 3-sided pyramidal facets occur on the bcc(111) surface after annealing to higher temperatures. Above $T_d \approx 870\text{K}$ the pyramids disappear and surface becomes flat. Attempts to freeze a high-temperature flat phase ended up with a faceted surface even for 60 K/s of cooling rate.

Another interesting property of faceting found in the present MC simulation is the dependence of T_d on the surface curvature. The temperature of transition T_d on a flat surface is smaller than T_d on a curved surface. In FEM experiment¹⁴, faceting of a Mo emitter covered by Pd has been observed in temperature range $750 - 1040\text{K}$, so at temperatures above $T_d \approx 870\text{K}$ for the Pd/Mo(111) system³. However, this can not be regarded as the evidence for higher defaceting temperature in a curved system because FEM observations were made at room temperature and the cooling effect could affect these FEM results.

Acknowledgements

We would like to thank dr Andrzej Szczepkowicz for discussions and help in preparing images.

-
- ¹ C.-Z. Dong, J. Guan, R. A. Campbell, T. E. Madey, in: X. Xie, S. Y. Tong, M. A. van Hove (Eds.), *The Structure of Surface IV*, World Scientific, Singapore, 1994, p. 328.
- ² C.-Z. Dong, L. Zhang, U. Diebold, T. E. Madey, *Surf. Sci.* 322 (1995) 221.
- ³ Ker-Jar Song, J. C. Lin, M. Y. Lai, Y. L. Wang, *Surf. Sci.* 327 (1995) 17.
- ⁴ T. E. Madey, J. Guan, C.-H. Nien, C.-Z. Dong, H.-S. Tao, R. A. Campbell, *Surf. Rev. Lett.* 3 (1996) 1315.
- ⁵ C.-H. Nien, T. E. Madey, *Surf. Sci.* 380 (1997) L527.
- ⁶ T. E. Madey, C.-H. Nien, K. Pelhos, J. J. Kolodziej, I. M. Abdelrehim, H.-S. Tao, *Surf. Sci.* 438 (1999) 191.
- ⁷ C.-H. Nien, T. E. Madey, Y. W. Tai, T. C. Leung, J. G. Che, C. T. Chan, *Phys. Rev. B* 59 (1999) 10335.
- ⁸ J. G. Che, C. T. Chan, C. H. Kuo, T. C. Leung, *Phys. Rev. Lett.* 79 (1997) 4230.
- ⁹ C. T. Chan, J. G. Che, T. C. Leung, *Progress in Surface Science* 59 (1998) 1.
- ¹⁰ A. Szczepkowicz, A. Ciszewski, *Surf. Sci.* 515 (2002) 441.
- ¹¹ A. Szczepkowicz, R. Bryl, *Surf. Sci.* 559 (2004) L169.
- ¹² A. Szczepkowicz, R. Bryl, *Phys. Rev. B* 71 (2005) 113416.
- ¹³ K. Pelhos, T. E. Madey, R. Błaszczyszyn, *Surf. Sci.* 426 (1999) 61.
- ¹⁴ G. Antczak, T. E. Madey, M. Błaszczyszyn, R. Błaszczyszyn, *Vacuum* 63 (2001) 43.
- ¹⁵ G. Antczak, R. Błaszczyszyn, T. E. Madey, *Prog. Surf. Sci.* 74 (2003) 81.
- ¹⁶ A.C. Levi, M. Kotrla, *J. Phys.: Condens. Matter* 9 (1997) 299.
- ¹⁷ K. Sasaki, *Surf. Sci.* 318 (1994) L1230.
- ¹⁸ H. van Beijeren, *Phys. Rev. Lett.* 38 (1977) 993.
- ¹⁹ G. Mazzeo, E. Carlon, H. van Beijeren, *Phys. Rev. Lett.* 74 (1995) 1391.
- ²⁰ S. Prestipino, G. Santoro, E. Tosatti, *Phys. Rev. Lett.* 75 (1995) 4468.
- ²¹ G. Santoro, M. Vendruscolo, S. Prestipino, E. Tosatti, *Phys. Rev. B* 53 (1996) 13169.
- ²² N.C. Bartelt, T.L. Einstein, E.D. Williams, *Surf. Sci.* 312 (1994) 411.
- ²³ V. P. Zhdanov, B. Kaseno, *Phys. Rev. B* 56 (1997) R10067.
- ²⁴ B. Salanon, F. Fabre, J. Lapujoulade, W. Selke, *Phys. Rev. B* 38 (1988) 7385.
- ²⁵ M. den Nijs, K. Rommelse, *Phys. Rev. B* 40 (1989) 4709.
- ²⁶ D. L. Woodraska, J. A. Jaszczak, *Phys. Rev. Lett.* 78 (1997) 258.
- ²⁷ C. Oleksy, *Surf. Sci.* 549 (2004) 246.
- ²⁸ D.P. Landau, K. Binder, *A Guide to Monte Carlo Simulation in Statistical Physics*, Cambridge University Press (2000).
- ²⁹ K. Binder, D.W. Heermann, *Monte Carlo Simulation in Statistical Physics*, Springer-Verlag (Berlin, 1988).
- ³⁰ A. Szczepkowicz, A. Ciszewski, R. Bryl, C. Oleksy, C.-H. Nien, Q. Wu, and T. E. Madey, submitted to *Surface Science* (2005).